Journal of Ceramic Processing Research. Vol. 17, No. 5, pp. 430~433 (2016)

J O U R N A L O F
Ceramic Processing Research

Photoluminescence properties of $Sr_{6-x}BP_5O_{20}:xEu^{2+}$ phosphors for white LED applications

D. A. Hakeem and K. Park*
Faculty of Nanotechnology and Advanced Material Engineering, Sejong University, Seoul 143-747, Korea

$Sr_{6-x}BP_5O_{20}:xEu^{2+}$ ($0.005 \le x \le 0.08$) bluish-green phosphors are prepared by solution combustion method. The photoluminescence excitation spectra show a broad band covering 250-450 nm with a maximum intensity at 353 nm, which matches well with the emission of ultraviolet LED chips. Upon 353 nm excitation, the photoluminescence emission spectra contain two distinct broad emission bands at 408 and 480 nm, which originate from the $4f^65d^1 \rightarrow 4f^7$ transitions of Eu^{2+} ions in $Sr_3(PO_4)_2 : Eu^{2+}$ and $Sr_{6-x}BP_5O_{20} : xEu^{2+}$, respectively. The emission intensities at 408 and 480 nm increase with increasing Eu^{2+} contents up to 5 and 2 mol%, respectively, and then decreased with further its contents.

Key words: White LEDs, Eu^{2+}-doped phosphor, 4f-5d transition, $Sr_{6-x}BP_5O_{20} : xEu^{2+}$.

Introduction

White light-emitting diodes (LEDs) have been widely used in full-color panel displays, solid-state lighting, and backlighting because of a high luminescent efficiency, long lifetime, and good environmental consideration [1-4]. In general, white LEDs have been fabricated by combining a blue LED chip emitting at ~ 460 nm and a yellow $Y_3Al_5O_{12} : Ce^{3+}$ phosphor [5]. To achieve intense white-light emission, the phosphor needs strong absorption of ultraviolet (UV) or blue radiation from an LED chip, high thermal stability, high luminescence quenching temperature, and good chemical stability.

Strontium borophosphate, $Sr_6BP_5O_{20}$, is considered a promising host material due to high quantum efficiency and low synthesis temperature [6]. Murakami *et al*. [7] prepared $Sr_{6-x}BP_5O_{20} : xEu^{2+}$ phosphors by heating the mixture of strontium phosphate, strontium carbonate, boric acid, and europium oxide at 1100-1200 °C under weak reducing atmosphere. The phosphors absorbed UV and blue radiations and emitted bluish-green light due to the 4f-5d transition of Eu^{2+}. Jung *et al*. [8] investigated the luminescence of $(Sr_{1-x-y}\ Ca_xBa_y)_2P_2O_7 : Eu^{2+}$ ($0.32 < x < 0.72$, $y < 0.04$) phosphors. The luminescence of the phosphors reached 70% of a commercially available $BaMgAl_{10}O_{17} : Eu^{2+}$ (BAM : Eu^{2+}) phosphor at 254 nm excitation. The color chromaticity was in the deep blue region, $x = 0.15$ and $y = 0.05$. Zhang *et al*. [9] reported bluish-green emission of the $Sr_6BP_5O_{20} : Eu^{2+}$ phosphor prepared by solid-state reaction method under weak reductive atmosphere. The excitation spectra showed a broad band covering 290 to 365 nm with a shoulder around 390 nm. Combining with GaInN based near-UV LEDs, a bluish-green LED was fabricated based on the $Sr_6BP_5O_{20}:Eu^{2+}$ phosphor. In addition, the time resolved luminescence and concentration quenching behavior of $Sr_6BP_5O_{20} : Eu^{2+}$ phosphors were studied by K.-S. Sohn [10]. The emission spectrum showed the superposition of two emission bands from Sr(I) and Sr(II) sites in $Sr_6BP_5O_{20}$. Shuanglong *et al*. [11] studied the photoluminescence of Mn^{2+} and Eu^{2+} co-doped $(Sr,Ba)_6BP_5O_{20}$ prepared by solid-state reaction method. The authors measured photoluminescence and color-coordinate parameters and investigated the effects of Ba^{2+} content on crystal structure and photoluminescence properties.

However, the photoluminescence properties of the above $Sr_{6-x}BP_5O_{20}:xEu^{2+}$ are not still enough for its practical applications as bluish-green phosphors. Therefore, in this study, to improve the photoluminescence properties of $Sr_{6-x}BP_5O_{20} : xEu^{2+}$ phosphors, we synthesized $Sr_{6-x}\ BP_5O_{20} : xEu^{2+}$ ($0.005 \le x \le 0.08$) phosphors with various Eu^{2+} contents by solution combustion method and studied the effect of Eu^{2+} content on the photoluminescence properties.

Experimental

A series of $Sr_{6-x}BP_5O_{20} : xEu^{2+}$ ($0.005 \le x \le 0.08$) phosphors was prepared by solution combustion method (Fig. 1). $Sr(NO_3)_2$, H_3BO_3, $(NH_4)_2HPO_4$, and Eu_2O_3 were used as starting materials. Citric acid ($C_3H_4(OH)(COOH)_3$) was used as a fuel for combustion and the ratio of metal nitrates to fuel was maintained as 1 : 1. Eu_2O_3 was reacted with HNO_3 to form $Eu(NO_3)_3$. The citric acid was dissolved in distilled water under stirring. A mixture of metal nitrates, H_3BO_3, $(NH_4)_2HPO_4$, and citric acid was then heated on hot plate at 120 °C for

*Corresponding author:
Tel : +82-2-3408-3777
Fax: +82-2-3408-4342
E-mail: kspark@sejong.ac.kr

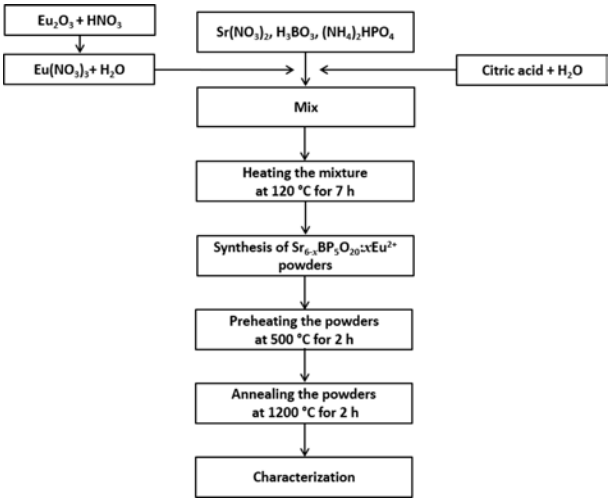

Fig. 1. A schematic diagram showing the preparation of $Sr_{6-x}BP_5O_{20}:xEu^{2+}$ ($0.005 \le x \le 0.08$) phosphors.

7 hrs. With the evaporation of the solution, intense heat was generated from the reaction of nitrates and citric acid to produce powders. The obtained powders were preheated at 500 °C for 3 hrs and then annealed at 1200 °C for 2 hrs under reductive carbon atmosphere with intermediate grinding. During the annealing, the reductive carbon atmosphere was applied for the reduction of Eu^{3+} to Eu^{2+}. The crystal structure of the annealed $Sr_{6-x}BP_5O_{20}:xEu^{2+}$ ($0.005 \le x \le 0.08$) phosphors was analyzed with an X-ray diffractometer (XRD; Rigaku RINT2000) with Cu Kα radiation ($\lambda = 0.15418$ nm). The photoluminescent spectra of the phosphors were obtained with a spectrofluorometer (QM-4/2005SE, PTI, USA) equipped with a 75 W Xenon lamp.

Results and Discussion

Fig. 2 shows the XRD patterns of the annealed $Sr_{6-x}BP_5O_{20}:xEu^{2+}$ ($0.005 \le x \le 0.08$) phosphors. The $Sr_{6-x}BP_5O_{20}:xEu^{2+}$ phosphors crystallized in tetragonal structure and I4c2 space group. The crystal structure consists of central [BO_4] tetrahedron surrounded by an array of [PO_4] tetrahedron [12-13]. Furthermore, there are two independent crystallographic cation sites Sr(I) and Sr(II) in the $Sr_6BP_5O_{20}$ host which are coordinated to eight and nine oxygen atoms, respectively [10, 14]. It is expected that the Eu^{2+} ions occupy the two Sr sites in the host lattice because of the similar ionic radius of Sr^{2+} (0.118 nm) and Eu^{2+} (0.129 nm) [9]. To the best of our knowledge, the Joint Committee on Powder Diffraction Standards (JCPDS) cards of $Sr_6BP_5O_{20}$ are not available. Therefore, we could not compare the XRD patterns obtained here with the JCPDS card of $Sr_6BP_5O_{20}$. A secondary phase $Sr_3(PO_4)_2$ with rhombohedral structure is detected, and its amount decreases with an increase in the Eu^{2+} content [12, 15, 16]. In addition, the XRD patterns do not contain any characteristic peaks originating from the Eu^{2+}, indicating that the Eu^{2+} is dissolved into the host

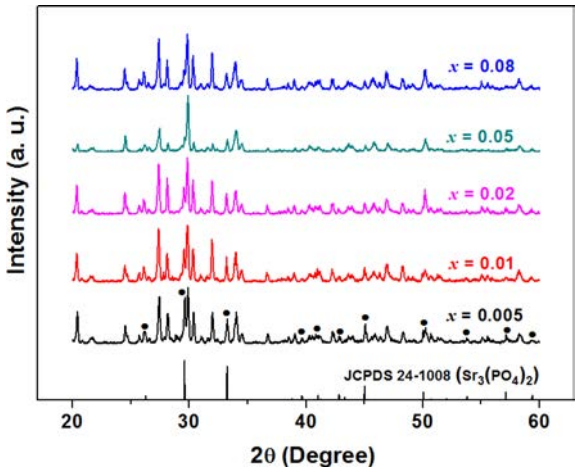

Fig. 2. XRD patterns of the $Sr_{6-x}BP_5O_{20}:xEu^{2+}$ ($0.005 \le x \le 0.08$) phosphors.

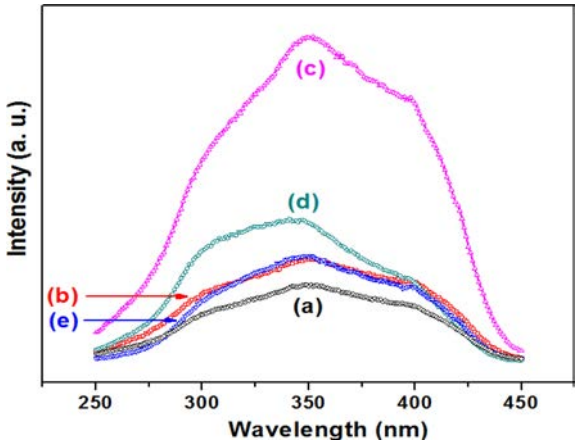

Fig. 3. Photoluminescence excitation spectra of the $Sr_{6-x}BP_5O_{20}:xEu^{2+}$ phosphors with different Eu^{2+} contents: x = (a) 0.005, (b) 0.01, (c) 0.02, (d) 0.05, and (e) 0.08.

lattice. The crystallite size (D) of the annealed $Sr_{6-x}BP_5O_{20}:xEu^{2+}$ ($0.005 \le x \le 0.08$) phosphors is calculated from the Scherrer formula: $D = (0.9\lambda)/(\beta\cos\theta)$, where λ is the wavelength of radiation, θ is the angle of the diffraction peak, and β is the full width at half maximum of the diffraction peak (in radian) [17]. The calculated crystallite sizes of the $Sr_{6-x}BP_5O_{20}:xEu^{2+}$ phosphors are 44.6, 46.3, 43.2, 40.7 and 45.5 for $x = 0.005$, 0.01, 0.02, 0.05 and 0.08, respectively.

The photoluminescence excitation spectra of $Sr_{6-x}BP_5O_{20}:xEu^{2+}$ ($0.005 \le x \le 0.08$) phosphors, monitored at 480 nm emission, are shown in Fig. 3. A strong broad absorption band is appeared in 250 to 450 nm at a maximum intensity of 353 nm. The excitation spectra consist of three absorption peaks centered at 297, 353 and 398 nm. The peaks centered at 353 and 398 nm could be assigned to the transitions of the Eu^{2+} ions from $4f^7$ ground state to the higher energy $4f^65d^1$ excited state and to the lower energy $4f^65d^1$ excited state, respectively [18]. In addition, the peak centered at 297 nm could be attributed to the host absorption and to the absorption of the secondary phase $Sr_3(PO_4)_2:Eu^{2+}$

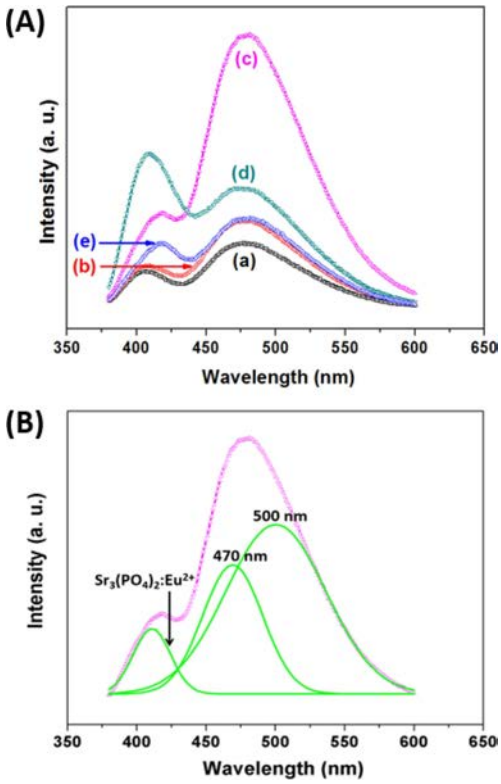

Fig. 4. (A) Photoluminescence emission spectra of the $Sr_{6-x}BP_5O_{20}:xEu^{2+}$ phosphors with different Eu^{2+} contents: x = (a) 0.005, (b) 0.01, (c) 0.02, (d) 0.05, and (e) 0.08. (B) Deconvoluted emission spectrum of $Sr_{5.98}BP_5O_{20}:0.02Eu^{2+}$ phosphor.

[16, 19]. The excitation intensity centered at 353 nm increases with an increase in the Eu^{2+} content up to 2 mol% and then decreases with further its contents. The strong excitation band at 353 nm suggests that the $Sr_{6-x}BP_5O_{20}:xEu^{2+}$ phosphors can be effectively excited by UV LED chips.

The photoluminescence emission spectra of $Sr_{6-x}BP_5O_{20}:xEu^{2+}$ ($0.005 \le x \le 0.08$) phosphors, monitored at 353 nm, contain two distinct broad emission peaks at 408 and 480 nm, as presented in Fig. 4(a). The broad asymmetric peak centered at 480 nm originates from the $4f^65d^1 \rightarrow 4f^7$ transition of Eu^{2+} ions. The emission spectra obtained here can be deconvoluted into two Gaussian curves centered at 470 and 500 nm. The two Gaussian curves of the $Sr_{5.98}BP_5O_{20}:0.02Eu^{2+}$ phosphor can be seen in Fig. 4(b). These results are quite similar to that studied by K.-S. Sohn [10]. These two Gaussians could be attributed to the coordination environment around the Eu^{2+} ions. The emissions at 470 and 500 nm are due to the transitions of Eu^{2+} ions at Sr(I) and Sr(II) sites, respectively [20]. There are two crystallographic Sr(I) and Sr(II) sites in the $Sr_{6-x}BP_5O_{20}:xEu^{2+}$ phosphors. The Sr(I) and Sr(II) sites are coordinated to eight and nine oxygen atoms, respectively. Furthermore, the emission peak at 408 nm is caused by the $4f^65d^1 \rightarrow 4f^7$ transition of Eu^{2+} ions in the secondary phase $Sr_3(PO_4)_2:Eu^{2+}$ [21]. It is found that the emission intensities centered at 408 and

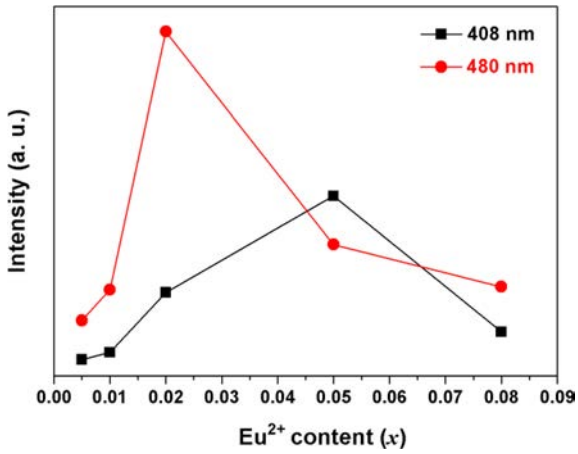

Fig. 5. Emission intensity at 408 and 480 nm wavelengths of the $Sr_{6-x}BP_5O_{20}:xEu^{2+}$ phosphors as a function of Eu^{2+} content.

480 nm for the $Sr_{6-x}BP_5O_{20}:xEu^{2+}$ ($0.005 \le x \le 0.08$) phosphors depend strongly on the Eu^{2+} content (Fig. 5). The emission intensities at 408 and 480 nm increase with increases in the Eu^{2+} contents up to 5 and 2 mol%, respectively, and then decrease with further its contents.

Conclusions

A series of $Sr_{6-x}BP_5O_{20}:xEu^{2+}$ ($0.005 \le x \le 0.08$) bluish-green phosphors was successfully prepared by the solution combustion method. The photoluminescence excitation spectrum showed a broad band from 250 to 450 nm with a maximum at 353 nm. Upon 353 nm excitation, two emission peaks at 408 and 480 nm were observed in the visible region from 380 to 600 nm. The photoluminescence emission peaks at 408 and 480 nm originated from the $4f^65d^1 \rightarrow 4f^7$ transitions of Eu^{2+} ions in $Sr_3(PO_4)_2:Eu^{2+}$ and $Sr_{6-x}BP_5O_{20}:xEu^{2+}$, respectively. The emission intensities at 408 and 480 nm increased with increasing the Eu^{2+} contents up to 5 and 2 mol%, respectively, and then decreased with further its contents.

References

1. W.-C. Ke, C.C. Lin, R.-S. Liu, and M.-C. Kuo, J. Electrochem. Soc. 157 (2010) J307-J309.
2. Z. Yang, G. Yang, S. Wang, J. Tian, X. Li, Q. Guo, and G. Fu, Mater. Lett. 62 (2008) 1884-1886.
3. A.S. Gouveia-Neto, N.P.S.M. Rios, and L.A. Bueno, Opt. Mater. 35 (2012) 126-129.
4. R.-J. Xie, N. Hirosaki, M. Mitomo, K. Sakuma, and N. Kimura, Appl. Phys. Lett. 89 (2006) 241103.
5. V.P. Dotsenko, S.M. Levshov, I.V. Berezovskaya, G.B. Stryganyuk, A.S. Voloshinovskii, and N.P. Efryushina, J. Lumin. 131 (2011) 310-315.
6. S. Su, W. Liu, R. Duan, L. Cao, G. Su, and C. Zhao, J. Alloys Compd. 575 (2013) 309-313.
7. K. Murakami, J. Narita, Y. Anzai, H. Itoh, S. Doi, and K. Awazu, J. Light Visual Environ. 3 (1979) 6-11.
8. Y.S. Jung, C. Kulshreshtha, J.S. Kim, N. Shin, and K.-S. Sohn, Chem. Mater. 19 (2007) 5309-5318.

9. M. Zhang, J. Wang, W. Ding, Q. Zhang, and Q. Su, Appl. Phys. B 86 (2007) 647-651.
10. K.-S. Sohn, S.H. Cho, S.S. Park, and N. Shin, Appl. Phys. Lett. 89 (2006) 051106.
11. Y. Shuanglong, C. Xianlin, Z. Chaofeng, Y. Yunxia, and C. Guorong, Opt. Mater. 30 (2007) 192-194.
12. K.-S. Sohn, J.G. Yoo, N. Shin, K. Toda, and D.-S. Zang, J. Electrochem. Soc. 152 (2005) H213-H218.
13. Y. Komatsu, A. Komeno, K. Toda, K. Uematsu, and M. Sato, J. Alloys Compd. 408-412 (2006) 903-906.
14. H. Ehrenberg, S. Laubach, P.C. Schmidt, R. McSweeney, M. Knapp, and K.C. Mishra, J. Solid State Chem. 179 (2006) 968-973.
15. N. Shin, J. Kim, D. Ahn, and K.-S. Sohn, Acta Crystallographica C 61 (2005) i54-i56.
16. S.H.M. Poort, J.W.H. van Krevel, R. Stomphorst, A.P. Vink, and G. Blasse, J. Solid State Chem. 122 (1996) 432-435.
17. A. Hakeem, K.N. Shinde, S.J. Yoon, S.J. Dhoble, and K. Park, J. Nanosci. Nanotechnol. 14 (2014) 5873-5876.
18. T. Cao, G. Chen, W. Lü, H. Zhou, J. Li, Z. Zhu, Z. You, Y. Wang, and C. Tu, J. Non-Cryst. Solids 355 (2009) 2361-2364.
19. F. Xiao, Y.N. Xue, and Q.Y. Zhang, Spectrochim. Acta Part A 74 (2009) 758-760.
20. Y. Qiao, X. Zhang, X. Ye, Y. Chen, and H. Guo, J. Rare Earths 27 (2009) 323-326.
21. S. Laubach, K.C. Mishra, K. Hofmann, B. Albert, P. Larsen, C. Wickleder, R. McSweeney, and P.C. Schmidt, J. Electrochem. Soc. 155 (2008) J205-J211.